Tirapazamine Cytotoxicity for Neuroblastoma Is p53 Dependent

Bo Yang[1,2,3] and C. Patrick Reynolds[1,3]

Abstract Relapse of neuroblastoma commonly occurs in hypoxic tissues, and is associated with an acquired and sustained high-level drug resistance, often due to p53 loss of function. Abrogating p53 function with HPV 16 E6 transduction in drug-sensitive neuroblastoma cell lines caused high-level drug resistance. Tirapazamine (TPZ) is a bioreductive agent that forms a toxic free radical in hypoxia. We determined in six neuroblastoma cell lines the cytotoxicity of TPZ using DIMSCAN, a digital imaging fluorescence assay, apoptosis and mitochondrial membrane potential ($\Delta\Psi_m$) by flow cytometry, and protein expression by immunoblotting. TPZ exhibited high cytotoxicity, especially in hypoxia (2% O_2), for all four p53-functional neuroblastoma cell lines, achieving >3 logs of cell kill ($LC_{99} \leq 0.7$ μg/mL). In p53-nonfunctional neuroblastoma cell lines, all TPZ LC_{99} values were >3.0 μg/mL (average clinically achievable level). TPZ (24 hours) induced apoptosis in >46% of cells in p53-functional cell lines but failed to cause apoptosis in p53 nonfunctional cell lines. Induction of p53 and p21 expression by TPZ was observed in a p53-functional cell line (SMS-SAN) but not in a p53-nonfunctional cell line (CHLA-90). Significant $\Delta\Psi_m$ loss and glutathione (GSH) depletion in response to TPZ was observed in p53-functional cell lines (SMS-SAN, SMS-SAN EV, and CHLA-15) but not in p53-nonfunctional cell lines (SMS-SAN E6 and CHLA-90). *N*-Acetylcysteine inhibited TPZ-mediated $\Delta\Psi_m$ loss and GSH depletion, but neither *N*-acetylcysteine nor Boc-d-fmk inhibited apoptosis caused by TPZ. In response to TPZ, $\Delta\Psi_m$ loss preceded apoptosis. Thus, TPZ cytotoxicity for neuroblastoma cell lines in hypoxia occurred via a p53-dependent mitochondrial pathway that caused induction of p53 and p21, $\Delta\Psi_m$ decrease, GSH depletion, and apoptosis. These data further define the mechanism of action of TPZ and suggest that as a single agent, TPZ would only have clinical activity against p53-functional neuroblastomas.

Bioreductive agents, such as Tirapazamine (TPZ), are preferentially cytotoxic in hypoxia and show activity against a variety of tumor cell lines (1–4). The toxic species has been inferred to be a hydroxyl radical that is produced by a cofactor-dependent, one-electron reduction of TPZ, catalyzed by various cellular reductases, including the flavoenzyme NADPH reductase (2, 5). This highly reactive radical can be detoxified by oxygen, but in hypoxia it is converted to a stable two-electron reduction product (known as SR4317) by reaction with cellular constituents. Exposure to TPZ under hypoxic conditions leads to increased reactive oxygen species (ROS), DNA strand breaks (single and double), chromosome aberrations, and cell death (3, 6). In hypoxia, TPZ enhanced the *in vitro* activity of radiation and alkylating agents (7–12). In clinical trials TPZ showed activity in combination with radiotherapy and cisplatin-based chemotherapy (13, 14).

Neuroblastoma is a common childhood tumor of the sympathetic nervous system (15–18). Treatment of high-risk neuroblastoma (stage IV patients >1 year old at diagnosis, and stage III disease with *MYCN* amplification and/or unfavorable histopathology) with myeloablative, multiagent chemoradiotherapy, supported with purged autologous bone marrow transplantation and followed by 13-*cis*-retinoic acid, has improved the outcome for high-risk neuroblastoma (16). However, >50% of high-risk neuroblastoma patients still ultimately die from progressive disease that is refractory to further therapy and is often associated with acquired loss of p53 function in the recurrent tumor cells (19). Because relapse of neuroblastoma commonly occurs in hypoxic sites (15), hypoxic tissue may serve as a "sanctuary" site for neuroblastoma (20), consistent with the hypoxia-mediated decrease in chemotherapy and radiotherapy activity reported for other tumor types (21, 22). Therefore, it is important to identify agents that both retain cytotoxicity in reduced-oxygen environments and are p53-independent for use in the treatment of neuroblastoma.

Because previous reports showed that TPZ was a p53-independent agent in non–small-cell lung cancer (23) and human squamous cell carcinoma of the tongue (24), we have examined the cytotoxic properties in hypoxia of TPZ against human neuroblastoma cell lines with and without p53 function. Here we report that TPZ only induced apoptosis, multi-log cytotoxicity, p53 and p21 overexpression, and loss of

Authors' Affiliations: [1]Developmental Therapeutics Program, USC-CHLA Institute for Pediatric Clinical Research, Division of Hematology-Oncology, Children's Hospital Los Angeles and Departments of [2]Pediatrics and [3]Pathology, Keck School of Medicine, University of Southern California, Los Angeles, California
Received 11/21/04; accepted 1/11/05.
Grant support: Neil Bogart Memorial Laboratories of the T.J. Martell Foundation for Leukemia, Cancer, and AIDS Research; National Cancer Institute grant CA82830; and Children's Hospital Los Angeles Research Institute Career Development Fellowship (B. Yang).
The costs of publication of this article were defrayed in part by the payment of page charges. This article must therefore be hereby marked *advertisement* in accordance with 18 U.S.C. Section 1734 solely to indicate this fact.
Requests for reprints: C. Patrick Reynolds, Developmental Therapeutics Program, USC-CHLA Institute for Pediatric Clinical Research, Children's Hospital, Los Angeles, MS#57, 4620 Sunset Boulevard, Los Angeles, CA 90027. Phone: 323-669-5646; Fax: 323-664-9226 or 9455; E-mail: preynolds@chla.usc.edu.

mitochondrial membrane potential ($\Delta\Psi_m$) in p53-functional neuroblastoma cell lines.

Materials and Methods

Human neuroblastoma cell lines. Five human neuroblastoma cell lines (25) were obtained from patients at various points of disease [three at diagnosis: SMS-SAN, SK-N-BE(1), and CHLA-15, all have functional p53 (19); two cell lines were derived at progressive disease during intensive multiagent chemotherapy: SK-N-BE(2) and CHLA-171, both p53-nonfunctiononal] and one cell line was derived at relapse after bone marrow transplantation (CHLA-90, p53-nonfunctional). SK-N-BE(1), SK-N-BE(2), and SMS-SAN were cultured in RPMI 1640 (Irvine Scientific, Santa Ana, CA) with 10% fetal bovine serum (FBS; Gemini Bio-Products, Inc., Calabasas, CA); CHLA-15, CHLA-171, and CHLA-90 were cultured in Iscove's modified Dulbecco's medium (BioWhittaker, Walkersville, MD) supplemented with 3 mmol/L L-glutamine, insulin, transferrin 5 μg/mL each, 5 ng/mL selenous acid (ITS Culture Supplement, Collaborative Biomedical Products, Bedford, MA), and 20% FBS (complete medium). All cell lines were cultured at 37°C in 5% CO_2 and were cultured without antibiotics to avoid drug interactions and to facilitate detection of *Mycoplasma*. Experiments were carried out at passages 15 to 30. Cells were detached from culture plates or flasks with the use of a modified Puck's Solution A plus EDTA (Puck's EDTA), which contains 140 mmol/L NaCl, 5 mmol/L KCl, 5.5 mmol/L glucose, 4 mmol/L $NaHCO_3$, 0.8 mmol/L EDTA (EDTA), 13 μmol/L phenol red, and 9 mmol/L HEPES buffer (pH 7.3; ref. 26).

The SMS-SAN EV cell line is a clone of SMS-SAN that was transduced with the LXSN retrovirus as an "empty vector" control and the SMS-SAN E6 cell line is a clone of SMS-SAN transduced with the *HPV16E6* gene carried in the LXSN retrovirus (19). Both lines are cultured in RPMI 1640 with 250 μg/mL G418 to select for gene incorporation; G418 is removed just before any drug testing (19).

Reduced oxygen conditions. For hypoxia assays, cells were cultured in plates or flasks and incubated in a sealed chamber with a mixture of 2% O_2, 5% CO_2, and 93% N (referred to as 2% O_2 mixture) at 37°C. Under these conditions, medium in plates and flasks attains a pO_2 of ~15 mm Hg (27). This level of oxygen is below the degree of hypoxia found in bone marrow (17) and in the range of hypoxia found in tumor tissue (28). TPZ stock solution was diluted in whole medium that had been allowed to equilibrate overnight in a loosely capped flask in the 2% O_2 chamber.

Chemicals. TPZ was provided by Sanofi-Winthrop, Inc. (Malvern, PA) and was dissolved just before use in sterile water to make a 1 mg/mL stock solution. L-Buthionine sulfoximine was obtained as a 50 mg/mL solution from the Investigational Drug Branch, National Cancer Institute (Rockville MD) and was diluted to various concentrations in complete medium. Eosin Y, Ploybrene (hexadimethrine bromide), and the thiol antioxidant *N*-acetylcysteine were purchased from Sigma Chemical Co. (St. Louis, MO). *N*-Acetylcysteine was freshly dissolved in medium at a final concentration of 500 μmol/L, the pH adjusted to 7.4 with NaOH, and sterilized by 0.22 μmol/L filtration. Fluorescein diacetate was from the Eastman Kodak Company (Rochester, NY). The mitochondrial fluorescent probe 5,5′, 6,6′-tetrachloro-1,1′,3,3′-tetraethylbenzimidazol-carbocyanine iodide (JC-1) was purchased from Molecular Probes (Eugene, OR). Boc-d-fmk was purchased from Enzyme System Products (Livemore, CA). Stock solutions of fluorescein diacetate (1 mg/mL), Boc-d-fmk (40 mmol/L) and JC-1 (2 mg/mL) were dissolved in dimethyl sulfoxide and stored at −20°C. Antibodies to p53 (DO-1) mouse monoclonal, p21 (C-19) rabbit polyclonal, Bcl-2 (100) mouse monoclonal, Bcl-xL (H-62) rabbit polyclonal, Bax (p-19) rabbit polyclonal, α-tubulin mouse monoclonal, and horseradish peroxidase (HRP)–labeled secondary antimouse and anti-rabbit antibodies were purchased from Santa Cruz Biotechnology, Inc. (Santa Cruz, CA). Enhanced chemiluminescence (ECL) Western blotting detection reagents were purchased from Amersham Pharmacia Biotech (Piscataway, NJ).

Cytotoxicity assay. All cytotoxicity assays are done in 96-well plates using a semiautomated digital image microscopy (DIMSCAN) system that has a dynamic range of 4 logs of cell kill (29). CHLA-15, CHLA-90, CHLA-171, and SK-N-BE(2) cells (fast growing) were plated at 5,000 cells per well; SK-N-BE(1), SMS-SAN, SMS-SAN EV (empty vector), and SMS-SAN E6 (HPV 16 E6 transduction) cells (slower growing) were plated at 15,000 cells per well; all cell lines were seeded in 100 μL of complete medium per well. Cells were cultured in hypoxia (2% O_2) and were allowed to attach 1 day before the addition of TPZ (0-2 μg/mL) in complete medium (to various final concentrations in 200 μL of complete medium) in replicates of 12 wells per condition. For some assays, *N*-acetylcysteine was added to a final concentration of 500 μmol/L, 3 hours before the addition of TPZ. Plates were assayed at 5 days after initiation of drug exposure.

To measure cytotoxicity, fluorescein diacetate was added to the 96-well plate (final concentration, 10 μg/mL) and incubated for 20 minutes. Afterwards 30 μL of eosin-Y (0.5% in normal saline) were added to quench background fluorescence of fluorescein diacetate in the medium and in nonviable cells (25). Total fluorescence per well (after digital thresholding to further eliminate background fluorescence) was then measured using a DIMSCAN system and results were expressed as the fractional survival of treated cells compared with control cells. The concentration of drug lethal for 99% of cells (LC_{99}) was calculated using the software "Dose-Effect Analysis with Microcomputers" (30).

Apoptosis. To quantify apoptotic cells with sub-G_0 DNA content, cells were cultured in complete medium in 25-cm^2 flasks, with or without 2 μg/mL TPZ for 24 hours in 2% O_2. Cells were then harvested, washed in PBS, centrifuged, and resuspended in 1 mL of 0.1% sodium citrate containing 0.05 mg propidium iodide and 50 μg RNase for 30 minutes at room temperature in the dark. RNase was dissolved in 10 mmol/L Tris-Cl (pH 7.5) and 15 mmol/L NaCl to a concentration of 10 mg/mL, and boiled at 100°C for 15 minutes, then stored in −20°C. DNA content was measured with a Coulter Epics Elite flow cytometer using a 488 nm argon laser and a 610 ± 10 nm band pass filter (20, 31).

Glutathione. Intracellular glutathione (GSH) was measured in triplicate by culturing cells in 25-cm^2 tissue culture flasks (2×10^2 cells) with or without 2 μg/mL TPZ for 24 hours in 2% O_2. For some assays, *N*-acetylcysteine was added to a final concentration of 500 μmol/L, 3 hours before the addition of TPZ. Cells were analyzed for total GSH content within 48 hours by the 5,5-dithiobis(2-nitrobenzoic acid)-oxidized GSH reductase method (32) as previously described (20, 33).

Assessment of mitochondrial potential transition. Loss of mitochondrial membrane potential ($\Delta\Psi_m$) leads to release of cytochrome *C* and other factors that trigger apoptosis (34, 35). The $\Delta\Psi_m$ was determined (36) in the SMS-SAN, SMS-SAN EV, SMS-SAN E6, CHLA-15, and CHLA-90 cell lines after a 24-hour treatment with 2 μg/mL TPZ in 2% O_2. For some assays, *N*-acetylcysteine was added to a final concentration of 500 μmol/L, 3 hours before the addition of TPZ. After collection with Puck's EDTA, cells were resuspended in 1 mL of complete medium containing 10 μg/mL of JC-1 for 10 minutes at 37°C. JC-1 is a cationic dye that exhibits potential-dependent accumulation in mitochondria (36), indicated by a fluorescence emission shift from green (525 ± 10 nm) to red (610 ± 10 nm). Cells (15,000 per sample) were analyzed by flow cytometry using an argon laser (488 nm). Mitochondria depolarization is specifically indicated by a decrease in the red to green fluorescence intensity ratio. The ratio in the control group was considered as 1.0.

Protein expression. Proteins were extracted in radioimmunoprecipitation assay buffer (50 mmol/L NaCl, 50 mmol/L Tris, 1% Triton X-100, 1% sodium deoxycholate, and 0.1% SDS) and 50 μg of total protein were loaded per lane. Proteins were fractionated on 12% Tris-glycine precast gels (Novex, San Diego, CA), transferred to

nitrocellulose membrane (Protran, Keene, NH), and probed with primary antibodies and then with HRP-labeled secondary antibodies. Antibody-positive bands were visualized using ECL Western blotting detection reagents.

Statistics. Significance (unpaired two-sided Student's *t* test) was determined by Microsoft Excel 2000 software.

Results

Cytotoxicity assays of tirapazamine under normoxia and hypoxia. The dose response of human neuroblastoma cell lines to TPZ (0-2 μg/mL) as a single agent in hypoxia (2% O_2) is shown in Fig. 1 and LC_{99} values are shown in Table 1. TPZ achieved >1 log (0.25 μg/mL) and >3 logs (2 μg/mL) of cell kill in all four p53-functional cell lines [SMS-SAN, CHLA-15, and SK-N-BE(1), and in SMS-SAN transduced with the LXSN empty vector (SMS-SAN EV)]. TPZ LC_{99} values for p53-functional cell lines in hypoxia (0.3-0.7 μg/mL; mean, 0.5 ± 0.2 μg/mL) were below clinically achievable steady-state plasma concentrations (2.88 ± 0.37 μg/mL; ref. 37). However, TPZ induced <1 log cell kill in four p53-nonfunctional cell lines: SK-N-BE(2),CHLA-90 (*TP53* mutated), CHLA-171 (*TP53* wild-type but nonfunctional), and SMS-SAN E6 (in which p53 function was abrogated by transduction of 16E6 HPV). The LC_{99} values for TPZ in all p53-nonfunctional cell lines (mean, >42.6 μg/mL; range, 20.6 to > 50 μg /mL) were greater than the reported clinically achievable steady-state plasma concentrations for TPZ of 2.88 ± 0.37 μg/mL (37).

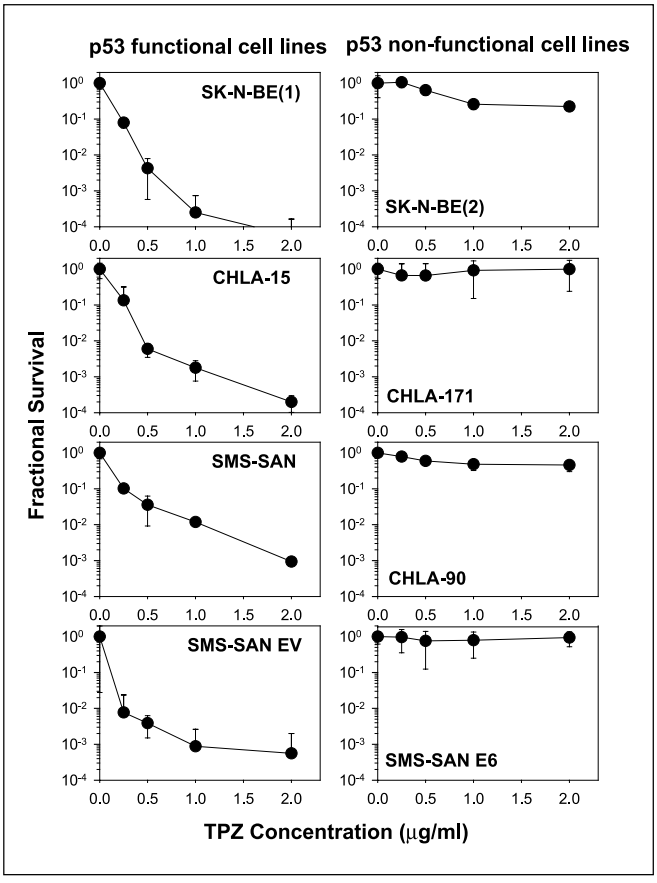

Fig. 1. Dose response of neuroblastoma cell lines to TPZ in hypoxia (2% O_2). Cells were treated with TPZ (0.25-2.0 μg/mL) for 5 days in the oxygen tensions indicated and cytotoxicity was analyzed with a fluorescence-based assay employing digital imaging microscopy (DIMSCAN). Cytotoxicity of TPZ was observed only in p53-functional cell lines. Points, mean fractional survival; bars, SD.

Table 1. Cytotoxicity of TPZ in hypoxia (2% O_2)

Cell line	p53 function	TPZ LC_{99} (μg/mL)
SK-N-BE(1)	+	0.4
CHLA-15	+	0.6
SMS-SAN	+	0.7
SMS-SAN EV	+	0.3
		Mean = 0.5 ± 0.2
SMS-SAN E6	−	>50
SK-N-BE(2)	−	20.6
CHLA-90	−	>50
CHLA-171	−	>50
		Mean > 42.7

NOTE: Concentration of TPZ required to achieve 99% cytotoxicity (LC_{99}). All data obtained from 5 days of TPZ exposure. +, p53 function; −, p53-nonfunctional. The mean LC_{99} for p53-functional cell lines was significantly different than that seen with p53-nonfunctional cell lines ($P < 0.001$).

Apoptosis following treatment with tirapazamine. The SMS-SAN cell line was treated with 2 μg/mL of TPZ for 24 hours and examined for apoptosis by propidium iodide staining and flow cytometry. Spontaneous apoptosis (control) was seen in 3% to 11% of cells in hypoxia (Fig. 2*A*). In 2% O_2, TPZ induced apoptosis in 65% (SMS-SAN) and 46% (SMS-SAN EV) of cells at 24 hours, but TPZ did not increase apoptosis (relative to controls) in the p53 nonfunctional cell lines SMS-SAN E6 and CHLA-90.

Expression of p53, p21, Bcl-2, Bcl-xL, and Bax. The basal and TPZ-treated expression of p53, p21, Bcl-2, Bcl-xL, and Bax was measured by immunoblotting. As shown in Fig. 2*B*, 2 μg/mL TPZ increased p53 and p21 protein levels in SMS-SAN cells after 24 hours of exposure in 2% O_2. In CHLA-90 (a *TP53*-mutated cell line with high basal p53 expression), TPZ (2 μg/mL) failed to increase p53 and p21 expression in 2% O_2. Increased expression of Bcl-2, Bcl-xL, or Bax was not detected in either the CHLA-90 or SMS-SAN cell lines after 2 μg/mL TPZ treatment for 24 hours.

Effect of tirapazamine on glutathione. Cell lines were incubated for 24 hours with 2 μg/mL TPZ in hypoxia and total GSH was assayed. TPZ induced a significant decrease in GSH to <70% baseline (Fig. 3*A*, $P < 0.05$) in four neuroblastoma cell lines with p53 function [SMS-SAN, SMS-SAN EV, CHLA-15, and SK-N-BE(1)], but not in the p53 nonfunctional, highly drug-resistant cell lines [SMS-SAN E6, SK-A-BE(2), CHLA-90, and CHLA-171; $P > 0.05$]. *N*-Acetylcysteine (500 μmol/L) significantly increased ($P < 0.05$) the basal level of GSH and restored TPZ-mediated GSH depletion in the CHLA-15 cell line (Fig. 3*B*), but failed to inhibit the cytotoxicity of TPZ (Fig. 3*C*).

Loss of mitochondrial membrane potential ($\Delta\Psi_m$). We determined $\Delta\Psi_m$ in SMS-SAN, SMS-SAN EV, SMS-SAN E6, CHLA-15, and CHLA-90 cell lines treated with 2 μg/mL of TPZ for 24 hours in hypoxia. Using flow cytometry, we measured $\Delta\Psi_m$ by JC-1 staining. TPZ decreased $\Delta\Psi_m$ in SMS-SAN, SMS-SAN EV, and CHLA-15 at 24-hour incubation (Fig. 4*A*), but failed to induce a loss of $\Delta\Psi_m$ in SMS-SAN E6 and CHLA-90. Consistent with the inability of *N*-acetylcysteine to inhibit TPZ cytotoxicity (Fig. 3*C*), *N*-acetylcysteine (500 μmol/L) failed to restore

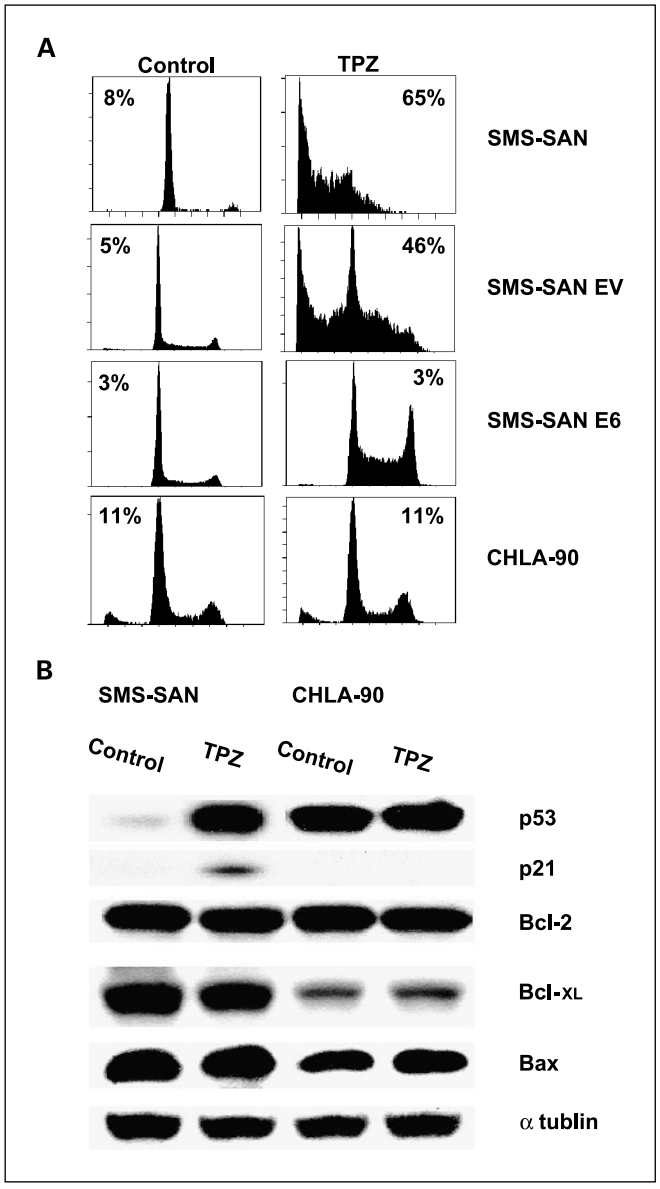

Fig. 2. Apoptosis and overexpression of p53 and p21, not Bcl-2, Bcl-xL, and Bax, were induced by TPZ. Neuroblastoma cell lines were treated with 2 μg/mL TPZ in hypoxia (2% O_2) for 24 hours. After treatment, cells were harvested with Puck's EDTA. *A,* apoptosis was assessed by propidium iodide staining of lysed cell nuclei (see Materials and Methods). The DNA content of 15,000 events was analyzed by flow cytometry. TPZ induced apoptosis only in p53-functional cell lines (SMS-SAN and SMS-SAN EV) but not in p53-nonfunctional cell lines (SMS-SAN E6 and CHLA-90). *B,* expression of p53, p21, bcl-2, and Bax was detected by Western blotting. Induction of p53 and p21 expression mediated by TPZ was observed in SMS-SAN but not in CHLA-90. TPZ failed to increase overexpression of Bcl-2, Bcl-xL, and Bax.

the $\Delta\Psi_m$ decrease caused by TPZ in CHLA-15 (Fig. 4*B*). The time course of apoptosis and $\Delta\Psi_m$ loss induced by TPZ showed that the $\Delta\Psi_m$ loss preceded the induction of apoptosis (Fig. 5*A*).

Effect of Boc-d-fmk on tirapazamine-induced apoptosis and loss of $\Delta\Psi_m$. To determine if TPZ-mediated apoptosis and loss of $\Delta\Psi_m$ in hypoxia are caspase dependent, we incubated CHLA-15 cells with the pan-caspase inhibitor Boc-d-fmk (40 μmol/L) for 1 hour before adding 2 μg/mL TPZ for 24 hours. Cells were treated with 500 μmol/L L-buthionine sulfoximine (20, 38) for 48 hours in normoxia (20% O_2) as a positive control for the ability of Boc-d-fmk to inhibit apoptosis. As shown in Fig 5*B*, Boc-d-fmk significantly ($P < 0.05$) inhibited L-buthionine sulfoximine–induced apoptosis in normoxia but failed ($P > 0.05$) to block TPZ-mediated apoptosis in hypoxia. Both L-buthionine sulfoximine and TPZ induced $\Delta\Psi_m$ decrease with or without Boc-d-fmk.

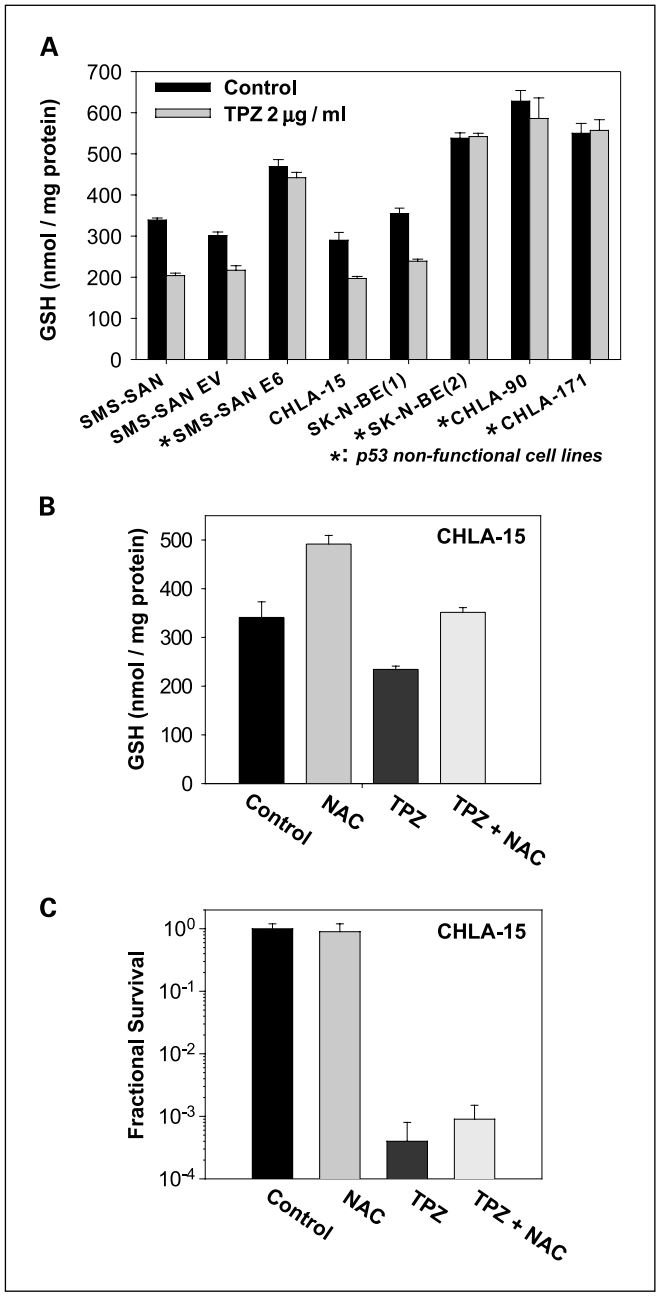

Fig. 3. The effect of TPZ [+/− *N*-acetylcysteine (*NAC*)] on intracellular GSH. Eight neuroblastoma cell lines were exposed for 24 hours (for GSH analysis) or 5 days (DIMSCAN cytotoxicity assay) in hypoxia (2% O_2) to 2 μg/mL TPZ. *N*-Acetylcysteine was added to a final concentration of 500 μmol/L, 3 hours before the addition of TPZ. Cells were harvested by Puck's EDTA, and then total GSH content was measured using the 5,5-dithiobis(2-nitrobenzoic acid)-oxidized GSH reductase method. *A,* TPZ significantly ($P < 0.05$) decreased GSH levels compared with corresponding controls in all p53-functional cell lines [SMS-SAN, SMS-SAN EV, SK-N-BE(1), and CHLA-15] but not ($P > 0.05$) in all p53-functional cell lines [SMS-SAN E6, SK-N-BE(2), CHLA-17, and CHLA-90]. *B,* *N*-acetylcysteine significantly reversed ($P < 0.01$) the GSH depletion but not the cytotoxicity ($P > 0.05$; *C*) induced by TPZ. Columns, mean of GSH levels; bars, SD.

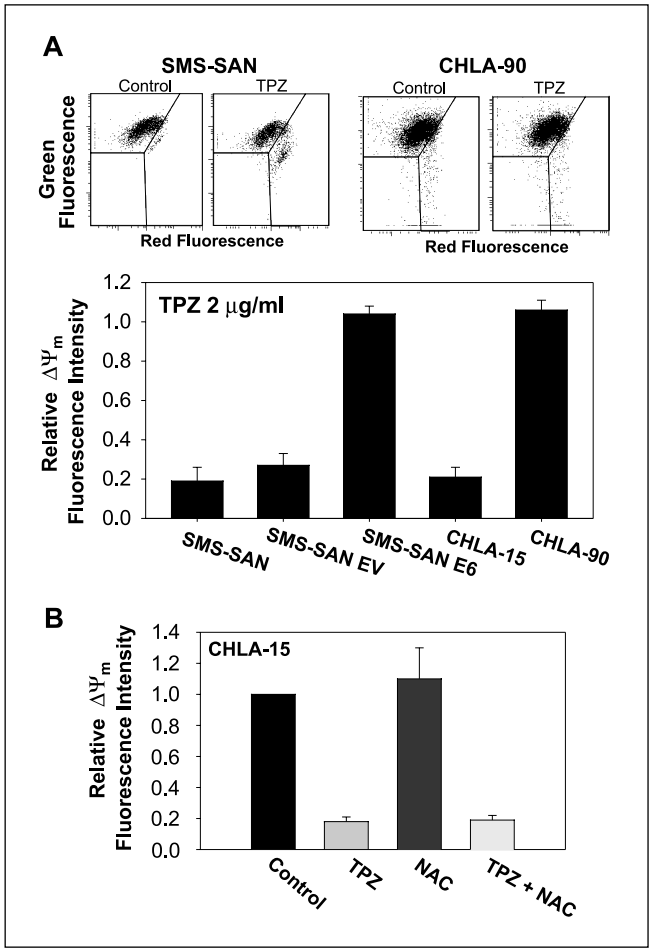

Fig. 4. Effect of TPZ (+/− *N*-acetylcysteine) on mitochondrial membrane potential ($\Delta\Psi_m$). Five cell lines were treated with 2 μg/mL TPZ for 24 hours in hypoxia (2% O_2). *N*-Acetylcysteine was added to a final concentration of 500 μmol/L, 3 hours before the addition of TPZ. Cells were harvested by Puck's EDTA and $\Delta\Psi_m$ was measured using the JC-1 dye (see Materials and Methods) in which mitochondria depolarization is indicated by a decrease in the red to green fluorescence intensity ratio. The ratio in the control group was considered as 1. *A,* TPZ significantly decreased $\Delta\Psi_m$ of p53-functional cell lines (SMS-SAN, SMS-SAN EV, and CHLA-15). *B,* *N*-acetylcysteine failed to restore TPZ-induced loss of $\Delta\Psi_m$ in CHLA-15.

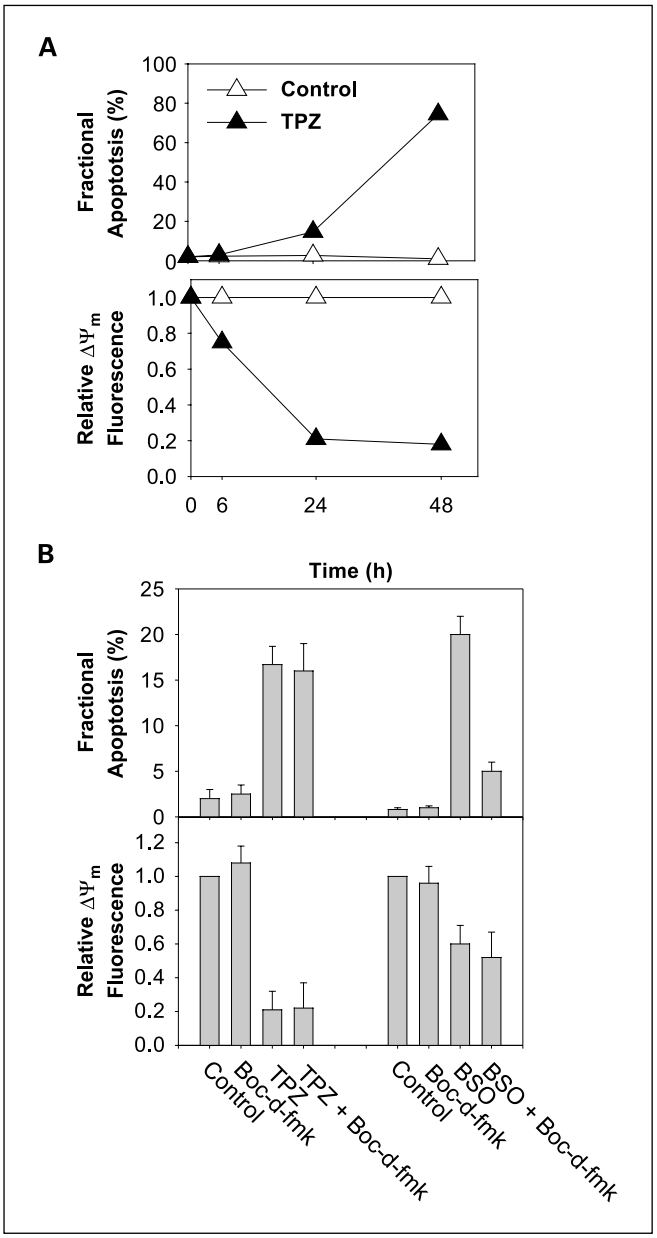

Fig. 5. Relationship between apoptosis and mitochondrial membrane potential $\Delta\Psi_m$ induced by TPZ and effect of Boc-d-fmk on them. *A,* time course of apoptosis and $\Delta\Psi_m$ loss induced by TPZ. CHLA-15 cells were treated with 2 μg/mL TPZ for 6, 24, and 48 hours in hypoxia (2% O_2) and collected to measure apoptosis and $\Delta\Psi_m$. A decrease in $\Delta\Psi_m$ (detected at 6 hours of treatment with TPZ) seemed to precede apoptosis (detected at 24 hours of treatment) induced by TPZ. *B,* Boc-d-fmk (refreshed every 24 hours) was added to a final concentration of 40 μmol/L, 1 hour before the treatment with 2 μg/mL TPZ (24 hours) in 2% O_2 or with 500 μmol/L L-buthionine sulfoximine (48 hours) in 20% O_2. Cells were treated with L-buthionine sulfoximine as a positive control for the ability of Boc-d-fmk to inhibit apoptosis. Boc-d-fmk significantly inhibited apoptosis induced by L-buthionine sulfoximine in normoxia ($P < 0.01$) but did not inhibit TPZ-mediated apoptosis in hypoxia ($P > 0.05$). Boc-d-fmk had no significant effect on $\Delta\Psi_m$ loss induced by TPZ and L-buthionine sulfoximine ($P > 0.05$).

Discussion

Neuroblastoma initially responds to chemotherapy but recurs in most high-risk patients as a chemotherapy-insensitive disease (15). Tumor hypoxia (found in common sites of neuroblastoma relapse, such as bone and bone marrow) could contribute to enhanced survival of tumor cells and facilitate selection for drug resistance (16–18). Because some chemotherapeutic agents are antagonized by hypoxia (1, 20, 22, 39), identifying regimens that are active in reduced oxygen environments could improve therapy for neuroblastoma.

TPZ is an anticancer drug that is activated in hypoxic cells to a highly damaging free radical, resulting in selective cytotoxicity of cells grown in hypoxia (5, 40). Preclinical models suggested that TPZ can enhance both irradiation and chemotherapy in hypoxic cancer cells (8–10), and previous reports indicated that TPZ is a p53-independent cytotoxic agent (23, 24). We showed that TPZ exhibited cytotoxicity only in p53-functional neuroblastoma cell lines. Clinically obtainable average levels of TPZ achieved 3 to > 4 logs of cell kill in all p53-functional cell lines with LC_{99} values ≤ 0.7 μg/mL, whereas all p53 nonfunctional cell lines showed high-level resistance to TPZ in hypoxia. The expression of p21 is transcriptionally activated by p53, and p21 mediates a p53-dependent G_1 arrest following

DNA damage, also potentially regulating chemosensitivity of tumor cells as a cell cycle checkpoint (41, 42). We found that TPZ induced expression of p53 and p21 proteins in SMS-SAN, a cell line established at diagnosis with functional p53 (19). However, in CHLA-90, a multidrug resistant cell line established after myeloablative therapy with mutated and nonfunctional *TP53* (19), basal and constitutive overexpression of p53 was observed, and p21 expression and apoptosis could not be induced by TPZ. These data suggested that TPZ is p53 dependent in neuroblastoma cell lines.

Because the p53-nonfunctional neuroblastoma cell lines are all derived after intensive chemotherapy and may possess drug resistance mechanisms beyond loss of p53 function, we studied the SMS-SAN E6 cell line in which p53 function was abrogated via HPV 16 E6 transduction (19). Unlike the SMS-SAN parental line, or empty vector controls, SMS-SAN E6 showed no response to TPZ in terms of apoptosis, $\Delta\Psi_m$ loss, or cytotoxicity. These data confirmed that TPZ cytotoxicity in neuroblastoma cell lines results from p53-dependent apoptosis. Our data contrast with previous reports that TPZ is a p53-independent bioreductive agent in non–small-cell lung cancer (23) and human squamous cell carcinoma of the tongue (24). The differences observed in TPZ cytotoxic behavior may be due to the different tumor cell types or the various dosages studied. The maximum dosage of TPZ we used is 2 μg/mL (11.2 μmol/L), which is below clinically achievable steady-state plasma concentrations (2.88 ± 0.37 μg/mL; ref. 37), but as hypoxic tumors are very likely to be only exposed to drug levels lower those achieved in plasma, we felt that 2 μg/mL was an appropriate maximum concentration for these experiments.

It has been shown that a change in mitochondrial membrane potential ($\Delta\Psi_m$) plays a pivotal role in transducing a variety of proapoptotic stimuli (43–45). Opening of permeability transition pores in mitochondria induces the release of cell death–promoting factors, including cytochrome *C* and apoptosis-inducing factor (35, 46). Cytochrome C has been shown to be involved in the activation of a caspase cascade (47, 48), whereas apoptosis-inducing factor has been shown to directly trigger apoptosis (49). Our time-course data showed that the TPZ-induced $\Delta\Psi_m$ loss preceded induction of apoptosis in hypoxic CHLA-15 cells, suggesting that the $\Delta\Psi_m$ loss may result in apoptosis in these p53-dependent cell lines. To show whether $\Delta\Psi_m$-mediated apoptosis is involved in caspase activation, we determined the effect of the pan-caspase inhibitor Boc-d-fmk on TPZ-induced $\Delta\Psi_m$ loss and apoptosis. The results showed that Boc-d-fmk significantly inhibited apoptosis induced by L-buthionine sulfoximine (a specific inhibitor of GSH synthesis; ref. 50) without an effect on the $\Delta\Psi_m$ decrease mediated by L-buthionine sulfoximine. Boc-d-fmk did not block TPZ-induced apoptosis or loss of $\Delta\Psi_m$. Taken together, the caspase inhibitor and time-course studies suggest that TPZ-induced apoptosis is mediated by mitochondrial permeability changes that lead to caspase-independent cytotoxicity.

It is reported that the release of mitochondrial apoptogenic factor is regulated by the pro- and anti-apoptotic Bcl-2 family proteins, which either induce or prevent the permeabilization of the outer mitochondrial membrane (51). *Bax* gene expression can be regulated *in vitro* by p53, and the ratio of Bax to Bcl-2 within a cell is critical for the cellular response to apoptotic stimuli (52). We showed that TPZ-induced apoptosis and $\Delta\Psi_m$ loss occurred only in p53-functional cell lines (SMS-SAN, SMS SAN EV, and CHLA-15) but not in p53-nonfunctional cell lines (CHLA-90 and SMS-SAN E6), suggesting that p53 activation may be essential for loss of $\Delta\Psi_m$, which then triggers apoptosis. However, TPZ-mediated p53 overexpression failed to change the expression of Bcl-2, Bcl-xL, and Bax proteins. Thus, further studies will be needed to address the actual link between TPZ-triggered p53 activation and the loss of $\Delta\Psi_m$ and the Bcl/Bax family of proteins.

Intracellular redox potential plays a role in the commitment to cell death, and a major determinant of the cellular redox state is GSH (43). GSH protects cells by detoxifying ROS, which are powerful activators of a decrease in $\Delta\Psi_m$ loss and apoptosis (43, 47, 53). Depletion of GSH is highly cytotoxic for neuroblastoma cell lines *in vitro* in standard culture conditions, likely due to unopposed ROS produced during catecholamine synthesis (38), and the protective effect of GSH in neuroblastoma can be replaced by antioxidants (20, 38), such as *N*-acetylcysteine. TPZ has been reported to induce ROS and cause DNA damage (3, 6, 20), and the elimination of ROS by *N*-acetylcysteine can inhibit p53-mediated apoptosis in some systems, suggesting a role for ROS in the p53 death response (54). Our data show that in p53-functional cell lines, TPZ significantly diminished GSH levels, $\Delta\Psi_m$, and cell survival. We also showed that *N*-acetylcysteine inhibited TPZ-mediated GSH depletion but not the loss of $\Delta\Psi_m$ or cytotoxicity induced by TPZ. *N*-Acetylcysteine could only partially decrease cytotoxicity of TPZ at low doses (<1 μg/mL, data not shown). Therefore, GSH depletion and ROS production do not seem to play essential roles in the p53-dependent cytotoxicity of TPZ for neuroblastoma cell lines.

Curiously, TPZ-mediated GSH depletion was only observed in p53-functional cell lines, and not in p53-nonfunctional lines, indicating that $\Delta\Psi_m$ loss and/or cytotoxicity may play a role in the decrease of GSH levels by TPZ. The ability of *N*-acetylcysteine to restore GSH without inhibiting $\Delta\Psi_m$ loss, cytotoxicity, or apoptosis suggests that the decreased GSH seen in p53-functional cell lines treated with TPZ was not simply due to a loss of cell viability. However, as p53-functional cell lines underwent significant apoptosis after 24 hours of TPZ treatment (Fig. 2), we cannot exclude death-related events as an explanation for the difference in GSH decrease seen in p53-functional compared with p53-nonfunctional cell lines.

Nearly half of the cell lines established from high-risk neuroblastomas recurring after intensive chemotherapy have *TP53* mutations and/or p53 loss of function (LOF; ref. 19). Whereas our data show that TPZ as a single agent is not effective against p53-LOF neuroblastoma cell lines, it is possible that combining TPZ with hypoxia-sensitive drugs that act in a p53-independent manner [examples include buthionine sulfoximine + melphalan (20) or fenretinide (27)] may result in a synergistic combination that is not limited by p53 function. However, our data suggest that use of TPZ may be best avoided in tumors in which loss of p53 function is common.

Acknowledgments

We thank Paul Alfaro for outstanding technical assistance.

References

1. Workman P, Stratford IJ. The experimental development of bioreductive drugs and their role in cancer therapy. Cancer Metastasis Rev 1993;12:73–82.
2. Saunders MP, Patterson AV, Chinje EC, Harris AL, Stratford IJ. NADPH:cytochrome *c* (P450) reductase activates tirapazamine (SR4233) to restore hypoxic and oxic cytotoxicity in an aerobic resistant derivative of the A549 lung cancer cell line. Br J Cancer 2000; 82:651–6.
3. Evans JW, Yudoh K, Delahoussaye YM, Brown JM. Tirapazamine is metabolized to its DNA-damaging radical by intranuclear enzymes. Cancer Res 1998;58: 2098–101.
4. Craighead PS, Pearcey R, Stuart G. A phase I/II evaluation of tirapazamine administered intravenously concurrent with cisplatin and radiotherapy in women with locally advanced cervical cancer. Int J Radiat Oncol Biol Phys 2000;48:791–5.
5. Patterson AV, Saunders MP, Chinje EC, Patterson LH, Stratford IJ. Enzymology of tirapazamine metabolism: a review. Anticancer Drug Des 1998;13: 541–73.
6. Dorie MJ, Kovacs MS, Gabalski EC, et al. DNA damage measured by the comet assay in head and neck cancer patients treated with tirapazamine. Neoplasia 1999;1:461–7.
7. Clement JJ, Gorman MS, Wodinsky I, Catane R, Johnson RK. Enhancement of antitumor activity of alkylating agents by the radiation sensitizer misonidazole. Cancer Res 1980;40:4165–72.
8. Goldberg Z, Evans J, Birrell G, Brown JM. An investigation of the molecular basis for the synergistic interaction of tirapazamine and cisplatin. Int J Radiat Oncol Biol Phys 2001;49:175–82.
9. Masunaga S, Ono K, Hori H, et al. Change in oxygenation status in intratumour total and quiescent cells following γ-ray irradiation, tirapazamine administration, cisplatin injection and bleomycin treatment. Br J Radiol 2000;73:978–86.
10. Jounaidi Y, Waxman DJ. Combination of the bioreductive drug tirapazamine with the chemotherapeutic prodrug cyclophosphamide for P450/P450-reductase–based cancer gene therapy. Cancer Res 2000;60:3761–9.
11. Wouters BG, Wang LH, Brown JM. Tirapazamine: a new drug producing tumor specific enhancement of platinum-based chemotherapy in non–small-cell lung cancer. Ann Oncol 1999;10 Suppl 5:S29–33.
12. Kovacs MS, Hocking DJ, Evans JW, Siim BG, Wouters BG, Brown JM. Cisplatin anti-tumour potentiation by tirapazamine results from a hypoxia-dependent cellular sensitization to cisplatin. Br J Cancer 1999;80:1245–51.
13. Craighead PS, Pearcey R, Stuart G. A phase I/II evaluation of tirapazamine administered intravenously concurrent with cisplatin and radiotherapy in women with locally advanced cervical cancer. Int J Radiat Oncol Biol Phys 2000;48:791–5.
14. Rischin D, Peters L, Hicks R, et al. Phase I trial of concurrent tirapazamine, cisplatin, and radiotherapy in patients with advanced head and neck cancer. J Clin Oncol 2001;19:535–42.
15. Reynolds CP, Seeger RC. Neuroblastoma. In Haskell CM, editors. Cancer Treatment, 5th ed. Philadelphia: W.B. Saunders; 2000. p. 1214–36.
16. Matthay KK, Villablanca JG, Seeger RC, et al. Treatment of high-risk neuroblastoma with intensive chemotherapy, radiotherapy, autologous bone marrow transplantation, and 13-*cis*-retinoic acid. Children's Cancer Group. N Engl J Med 1999;341:1165–73.
17. Grant JL, Smith B. Bone marrow gas tensions, bone marrow blood flow, and erythropoiesis in man. Ann Intern Med 1963;58:801–9.
18. Matthay KK, Atkinson JB, Stram DO, Selch M, Reynolds CP, Seeger RC. Patterns of relapse after autologous purged bone marrow transplantation for neuroblastoma: a Children's Cancer Group pilot study. J Clin Oncol 1993;11:2226–33.
19. Keshelava N, Zuo JJ, Chen P, et al. Loss of p53 function confers high-level multi-drug resistance in neuroblastoma cell lines. Cancer Res 2001;61:5103–5.
20. Yang B, Keshelava N, Anderson CP, Reynolds CP. Antagonism of buthionine sulfoximine cytotoxicity for human neuroblastoma cell lines by hypoxia is reversed by the bioreductive agent tirapazamine. Cancer Res 2003;63:1520–6.
21. Dachs GU, Tozer GM. Hypoxia modulated gene expression: angiogenesis, metastasis and therapeutic exploitation. Eur J Cancer 2000;36:1649–60.
22. Brown JM, Koong A. Therapeutic advantage of hypoxic cells in tumors: a theoretical study [see comments]. J Natl Cancer Inst 1991;83:178–85.
23. Wouters BG, Wang LH, Brown JM. Tirapazamine: a new drug producing tumor specific enhancement of platinum-based chemotherapy in non–small-cell lung cancer. Ann Oncol 1999;10 Suppl 5:S29–33.
24. Nagasawa H, Yamashita M, Mikamo N, et al. Design, synthesis and biological activities of antiangiogenic hypoxic cytotoxin, triazine-*N*-oxide derivatives. Comp Biochem Physiol A Mol Integr Physiol 2002; 132:33–40.
25. Keshelava N, Seeger RC, Groshen S, Reynolds CP. Drug resistance patterns of human neuroblastoma cell lines derived from patients at different phases of therapy. Cancer Res 1998;58:5396–405.
26. Reynolds CP, Biedler JL, Spengler BA, et al. Characterization of human neuroblastoma cell lines established before and after therapy. J Natl Cancer Inst 1986;76:375–87.
27. Maurer BJ, Metelitsa LS, Seeger RC, Cabot MC, Reynolds CP. Increase of ceramide and induction of mixed apoptosis/necrosis by *N*-(4-hydroxyphenyl)-retinamide in neuroblastoma cell lines. J Natl Cancer Inst 1999;91:1138–46.
28. Vaupel P, Schlenger K, Knoop C, Hockel M. Oxygenation of human tumors: evaluation of tissue oxygen distribution in breast cancers by computerized O2 tension measurements. Cancer Res 1991; 51:3316–22.
29. Proffitt RT, Tran JV, Reynolds CP. A fluorescence digital image microscopy system for quantifying relative cell numbers in tissue culture plates. Cytometry 1996;24:204–13.
30. Chou J, Chou TC. Dose effect analysis with microcomputers. Dose Effect Analysis with Microcomputers. Cambridge, UK: Elsevier-Biosoft; 1988.
31. Royall JA, Ischiropoulos H. Evaluation of 2′,7′-dichlorofluorescin and dihydrorhodamine 123 as fluorescent probes for intracellular H_2O_2 in cultured endothelial cells. Arch Biochem Biophys 1993;302: 348–55.
32. Vandeputte C, Guizon I, Genestie-Denis I, Vannier B, Lorenzon G. A microtiter plate assay for total glutathione and glutathione disulfide contents in cultured/isolated cells: performance study of a new miniaturized protocol. Cell Biol Toxicol 1994;10: 415–21.
33. Butturini A, Chen RL, Tang SQ, et al. Detection of bone marrow metastases in neuroblastoma by RT-PCR for neural and tumor associated genes. Proc Amer Soc Clin Oncol 1996;15:468.
34. Poulaki V, Mitsiades N, Romero ME, Tsokos M. Fas-mediated apoptosis in neuroblastoma requires mitochondrial activation and is inhibited by FLICE inhibitor protein and Bcl-2. Cancer Res 2001;61: 4864–72.
35. Susin SA, Zamzami N, Kroemer G. Mitochondria as regulators of apoptosis: doubt no more. Biochim Biophys Acta 1998;1366:151–65.
36. Mancini M, Anderson BO, Caldwell E, Sedghinasab M, Paty PB, Hockenbery DM. Mitochondrial proliferation and paradoxical membrane depolarization during terminal differentiation and apoptosis in a human colon carcinoma cell line. J Cell Biol 1997;138:449–69.
37. Shulman LN, Buswell L, Riese N, et al. Phase I trial of the hypoxic cell cytotoxin tirapazamine with concurrent radiation therapy in the treatment of refractory solid tumors. Int J Radiat Oncol Biol Phys 1999;44:349–53.
38. Anderson CP, Tsai JM, Meek WE, et al. Depletion of glutathione by buthionine sulfoxine is cytotoxic for human neuroblastoma cell lines via apoptosis. Exp Cell Res 1999;246:183–92.
39. Maurer BJ, Melton L, Billups C, Cabot MC, Reynolds CP. Synergistic cytotoxicity in solid tumor cell lines between *N*-(4-hydroxyphenyl)retinamide and modulators of ceramide metabolism. J Natl Cancer Inst 2000;92:1897–909.
40. Brown JM. SR 4233 (tirapazamine): a new anticancer drug exploiting hypoxia in solid tumours. Br J Cancer 1993;67:1163–70.
41. Hartwell LH, Kastan MB. Cell cycle control and cancer. Science 1994;266:1821–8.
42. Liu MC, Gelmann EP. P53 gene mutations: case study of a clinical marker for solid tumors. Semin Oncol 2002;29:246–57.
43. Hall AG. Review: The role of glutathione in the regulation of apoptosis. Eur J Clin Invest 1999;29: 238–45.
44. Kondo M, Oya-Ito T, Kumagai T, Osawa T, Uchida K. Cyclopentenone prostaglandins as potential inducers of intracellular oxidative stress. J Biol Chem 2001; 276:12076–83.
45. Serafino A, Sinibaldi-Vallebona P, Lazzarino G, et al. Modifications of mitochondria in human tumor cells during anthracycline-induced apoptosis. Anticancer Res 2000;20:3383–94.
46. Wilson MR. Apoptotic signal transduction: emerging pathways. Biochem Cell Biol 1998;76: 573–82.
47. Yang CF, Shen HM, Ong CN. Intracellular thiol depletion causes mitochondrial permeability transition in ebselen-induced apoptosis. Arch Biochem Biophys 2000;380:319–30.
48. Zou H, Li Y, Liu X, Wang X. An APAF-1.cytochrome *c* multimeric complex is a functional apoptosome that activates procaspase-9. J Biol Chem 1999;274: 11549–56.
49. Susin SA, Lorenzo HK, Zamzami N, et al. Molecular characterization of mitochondrial apoptosis-inducing factor. Nature 1999;397:441–6.
50. Tew KD, Houghton PJ, Houghton JA. Preclinical and clinical modulation of anticancer drugs. Preclinical and Clinical Modulation of Anticancer Drugs. Boca Raton: CRC Press; 1993. p. 13–7.
51. Schuler M, Green DR. Mechanisms of p53-dependent apoptosis. Biochem Soc Trans 2001;29: 684–8.
52. Brady HJ, Gil-Gomez G. Bax. The pro-apoptotic Bcl-2 family member, Bax. Int J Biochem Cell Biol 1998;30:647–50.
53. Bates S, Vousden KH. Mechanisms of p53-mediated apoptosis. Cell Mol Life Sci 1999;55: 28–37.
54. Johnson TM, Yu ZX, Ferrans VJ, Lowenstein RA, Finkel T. Reactive oxygen species are downstream mediators of p53-dependent apoptosis. Proc Natl Acad Sci U S A 1996;93:11848–52.